Rapid Communications

Abnormal phase flip in the coherent phonon oscillations of Ca_2RuO_4

Min-Cheol Lee,[1,2] Choong H. Kim,[1,2] Inho Kwak,[1,2] J. Kim,[3] S. Yoon,[3] Byung Cheol Park,[1,2] Bumjoo Lee,[1,2] F. Nakamura,[4] C. Sow,[5] Y. Maeno,[5] T. W. Noh,[1,2,*] and K. W. Kim[6,†]

[1]*Center for Correlated Electron Systems (CCES), Institute for Basic Science (IBS), Seoul 08826, Republic of Korea*
[2]*Department of Physics and Astronomy, Seoul National University, Seoul 08826, Republic of Korea*
[3]*Department of Physics and New Renewable Energy Research Center (NREC), Ewha Womans University, Seoul 03760, Republic of Korea*
[4]*Department of Education and Creation Engineering, Kurume Institute of Technology, Fukuoka 830-0052, Japan*
[5]*Department of Physics, Graduate School of Science, Kyoto University, Kyoto 606-8502, Japan*
[6]*Department of Physics, Chungbuk National University, Cheongju, Chungbuk 28644, Republic of Korea*

(Received 18 August 2018; revised manuscript received 28 September 2018; published 17 October 2018)

We employ an optical pump-probe technique to study coherent phonon oscillations in Ca_2RuO_4. We find that oscillation amplitude of an A_g symmetric phonon mode is strongly suppressed at 260 K, a putative transition point of orbital ordering. The oscillation also shows a gradual but huge change in its phase, such that the oscillation even flips over with a 180° change across the temperature. Density functional theory calculations indicate that the A_g phonon has an eigenmode of octahedral distortion with conventional tilting along the *a* axis and antipolar distortion of apical oxygen. Careful inspection of the lattice captures an unusually large antipolar distortion in low-temperature structures, which may play a crucial role for the phase transition at 260 K.

DOI: 10.1103/PhysRevB.98.161115

Ca_2RuO_4 is a prototype Mott insulator, where all of the degrees of freedom charge, spin, orbital, and lattice show robust interactions in distinctive phase transitions [1–8]. A metal-insulator transition (MIT) occurs at $T_{MIT} = 357$ K, accompanied by a structural transition that involves strong distortions of octahedral flattening and tilting [1,2]. Upon cooling, antiferromagnetic (AFM) spin ordering develops in Ca_2RuO_4 below $T_N = 113$ K, where its magnetism is determined by the spin-orbit coupling and the tetragonal distortions [3–5]. Recently, the sizable spin-phonon coupling has been observed in coherent phonon oscillations [6]. Another interesting anomaly has been observed below $T_{OO} = 260$ K, where an orbital ordering has been suggested. Resonant x-ray scattering (RXS) experiments indicated that the antiferromagnetic diffraction peak shows up even in the paramagnetic phase below T_{OO} [7,8]. However, the exact configuration and origin of the ordering remain unresolved. Apart from these RXS results, there have been no further experimental observations on the 260 K anomaly, nor has any theoretical model been presented to support the order.

Recent advances in ultrafast techniques have rendered it possible to investigate novel phenomena in nonequilibrium states [9–19]. Of particular interest is coherent phonon oscillations, which result in oscillations of a probing signal arising from periodic modulation of the lattice potential [19–22]. In contrast to thermally activated phonons with random *phase*s, coherent phonons provide an oscillation-phase value that reflects physical properties of a material. However, this phase tends to be overlooked, as it has been believed to be simply determined by the generation mechanism [19–22].

In this study, we find that the coherent phonon oscillations of Ca_2RuO_4 exhibit huge anomalies across T_{OO}. To our surprise, one A_g phonon mode changes its oscillation phase showing an unexpected 180° flip. Density-functional theory (DFT) calculations find that the A_g phonon mode is of octahedral tilting vibrations that are nearly parallel to the structural deformation at $T < T_{OO}$. Scrutiny of the temperature-0dependent octahedral structure reveals that a lattice deformation with a large antipolar distortion along the *b* axis develops below T_{OO}.

We perform time-resolved reflectance measurements on single-crystalline Ca_2RuO_4, synthesized by the floating zone method [23]. We utilize near infrared 800-nm pulses for both the pump and probe beams generated from a commercial Ti:sapphire amplifier system with a 250-kHz repetition rate. The corresponding photon energy of 1.55 eV is much greater than the optical gap of 0.6 eV of Ca_2RuO_4 [24]. The time duration of the pump and probe pulses are 30 fs. The oscillations show a linear response to pump fluence over a wide fluence range up to 1 mJ/cm^2 (Supplemental Material Fig. S1) [25]. We present data measured at pump and probe fluences of 140 and 80 μJ/cm^2, respectively, to minimize the heating effect and to maintain the measurement conditions close to the linear response region of the electronic response. The full width half maximum (FWHM) spot sizes of the pump and probe pulses were 80 and 40 μm, respectively. The pump and probe pulses are linearly polarized and perpendicular to each other. We cannot find a noticeable anisotropy of the response depending on both pump and probe polarizations.

We perform first-principles calculations based on fully relativistic DFT including spin-orbit coupling. We use the Perdew-Burke-Ernzerhof (PBE) form of the exchange-correlation functional, as implemented in the Vienna *Ab Initio* Simulation Package [26,27]. We use an $8 \times 8 \times 4$ *k*-point

*Corresponding author: twnoh@snu.ac.kr
†Corresponding author: kyungwan.kim@gmail.com

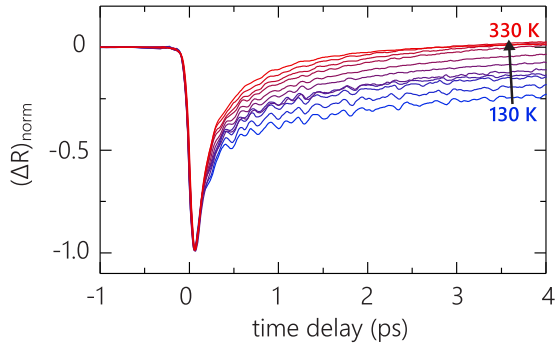

FIG. 1. Photoinduced reflectivity change normalized by maximum peaks for clarity. The photoinduced reflectivity transient is measured at every 20 K from 130 to 330 K.

mesh and a kinetic energy cut-off value of 500 eV. We adopt $U_{\text{eff}}(= U - J) = 2.5$ eV [28,29] to consider the local Hubbard interaction in Ru. For the structural relaxation, the Hellman-Feynman forces are converged to 0.5 meV/Å. To calculate the zone-center phonon mode, we use the frozen phonon method.

Figure 1 shows the photoinduced reflectivity change of Ca_2RuO_4 after near-infrared pumping at various temperatures from 130 to 330 K. The data are normalized by the maximum peak values at each temperature for a clear comparison. Analysis using a biexponential function fitting (Fig. S2) [25] indicates that relaxation processes exhibit two decay timescales of 0.1 and 1 ps. The electronic responses of both relaxation times do not show a noticeable anomaly across T_{OO}.

Superimposed over the overall relaxation, periodic oscillations in the transient reflectivity are clearly observed. The oscillating components obtained by subtracting the electronic responses by means of the biexponential curve fitting are shown in Fig. 2(a). Fourier transform analysis reveals that the coherent oscillations are composed of multiple phonon modes as shown in Fig. 2(b). All of the modes correspond to A_g symmetric phonons that have been observed in the previous Raman experiments [30,31]. Interestingly, the A_g phonon mode of the lowest frequency of 3.8 THz gets almost fully suppressed at $T \sim T_{\text{OO}} = 260$ K. The suppression also appears in Raman-scattering spectra as shown in Fig. S3 [25], although previous Raman studies did not focus on the transition at T_{OO} [30,31].

To extract quantitative information from the coherent oscillations, we fit the data with a damped harmonic oscillator model: $\Delta R_{CP}(t) = -\Sigma_i A_i \cos(2\pi f_i + \phi_i)\exp(t/\tau_i)$, where A_i, f_i, ϕ_i, and τ_i present the amplitude, frequency, initial phase, and damping time of the A_g symmetric modes, respectively. The fitting results are shown as line curves in Fig. 2(a); all of the curves are well matched to the measurement data. Figures 2(c) and 2(d) show the oscillation amplitude and phase of the 3.8 THz mode, respectively. Both parameters show clear anomalies, i.e., not only suppression of the amplitude, but also huge variation in the phase across T_{OO}. These anomalies show up also in the time domain signal of the A_g phonon oscillations of the lowest-frequency mode after the subtraction of higher-frequency components above 4 THz, as shown in Fig. 2(e). Such a phase variation by 180° of flipping is unexpected without a structural transition. As far as we know, the oscillation-phase flip has been reported

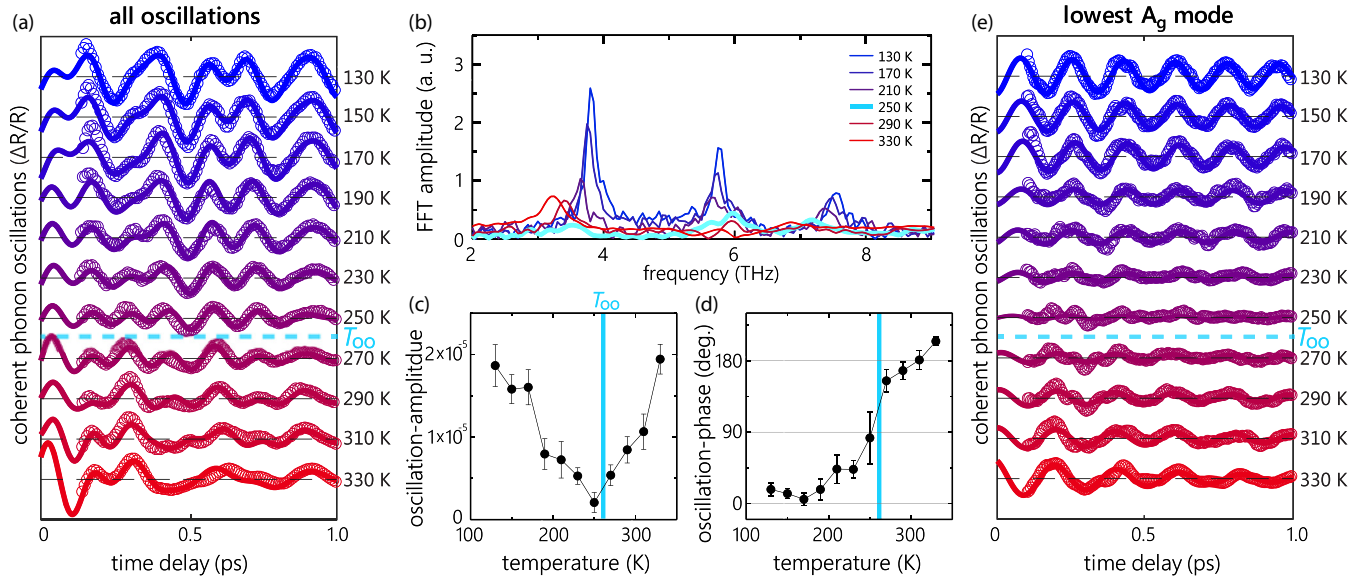

FIG. 2. (a) Coherent phonon oscillations of photoinduced reflectivity change (open circles). The data have been subtracted using a biexponential decay fitting (solid lines) at temperature intervals of 20 K from 130 to 330 K. These data are not normalized by maximum peaks. (b) Fourier transformation data of the oscillating components in (a). All oscillating components correspond to A_g symmetric Raman modes. (c),(d) T-dependent fitting parameters for the amplitude and phase of the lowest-frequency mode. (e) The oscillating component (open circles) and fit curves (solid lines) for the lowest-frequency mode. Higher-frequency oscillations have been subtracted from the raw data using the damped harmonic oscillator model fitting. The lowest A_g oscillation exhibits clear anomalies across $T_{\text{OO}} = 260$ K, where the amplitude is nearly suppressed and the oscillation *phase* changes with a 180° flip.

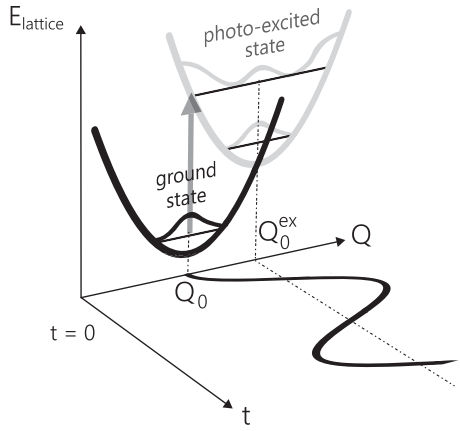

FIG. 3. Schematic diagram of conventional generation mechanism of displacive phonon oscillations. The arrow indicates the optical transition resulting from 1.55 eV pumping. Vibrational functions of $n = 0$ and $n = 1$ modes are also displayed in each lattice potential.

previously only once in blue bronze across a structural phase transition [16].

The observed phase values in Fig. 2(e) suggest that the cosine-type phonon oscillations are dominant in the paramagnetic insulating state well below and above T_{OO}. Such cosine-type oscillations have been explained by the displacive-type generation [20]. The generation process is shown schematically in Fig. 3 in terms of the lattice potential as a function of lattice coordinate (Q) depending on the absorption. The essence is that photoexcitation can shift the minimum position of the lattice potential from Q_0 to Q_0^{ex}, because of an instantaneous change in the charge density distribution [20–22]. Using optical ellipsometry techniques, we confirm that Ca_2RuO_4 are always strongly absorbing the pump beam at all measured temperatures (Fig. S4) [25], which is consistent with the displacive-type oscillations. Although there is a gradual change in absorption across T_{OO}, the 180° phase flip is unexpected based on the case of the above-mentioned displacive-type coherent phonons.

What is the origin of the phase flip in Ca_2RuO_4? Modulations of the reflectivity due to phonon oscillations should follow $\Delta R_{CP} = (\partial R/\partial Q)\delta Q$ [20–22]. The initial displacement δQ at $t = 0$ is determined by the shift of the minimum of the lattice potential, $Q_0^{ex} - Q_0$ in Fig. 3. If $\delta Q = Q_0^{ex} - Q_0$ gradually changes its sign, the flip of the reflectivity modulations may occur (Fig. S5) [25]. The gradual sign change of δQ is also consistent with the suppression of the oscillation amplitude when $\delta Q \sim 0$ around T_{OO}. On the other hand, the phase flip could occur when $(\partial R/\partial Q)$ changes the sign while δQ stays with the same sign. The change of the reflectivity on the phonon displacement is given by $\partial R/\partial Q = (\partial R/\partial \epsilon_1)(\partial \epsilon_1/\partial Q) + (\partial R/\partial \epsilon_2)(\partial \epsilon_2/\partial Q)$ [20]. The contributions of $(\partial \epsilon_1/\partial Q)^2$ and $(\partial \epsilon_2/\partial Q)^2$ are proportional to the Raman cross section [20], the intensity of which shows an anomaly across T_{OO} as illustrated in Fig. S3 [25]. Thus, it is also possible that Raman susceptibility changes sign across the ordering temperature, whereas the sign of the initial phonon displacement δQ is invariant.

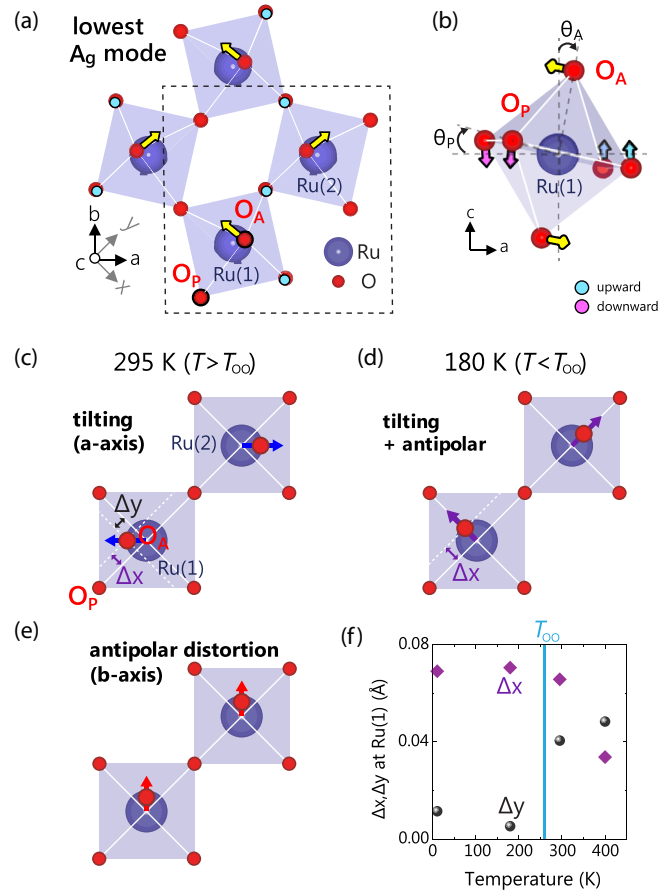

FIG. 4. (a),(b) Eigenmode of the lowest A_g phonon mode. The black arrows indicate vibrations of the apical oxygen atoms (O_A). The modulations of in-plane oxygen atoms (O_P) in upward (orange circle) and downward (sky-blue circle) directions have a magnitude comparable to that of O_A. The dotted box indicates the pair of neighboring RuO_6 octahedra which are described in (c)–(e) schematically. (c),(d) Simplified diagrams of the octahedral distortions (ignoring rotation) (c) above T_{OO} and (d) below T_{OO}. At 295 K ($> T_{OO}$), the difference in tilting angle between O_A and O_P causes shifts in the positions of O_P from the symmetric center positions. In particular, the structural distortions in (d) are nearly parallel to the eigenmode of the A_g phonon mode in (a). (e) Schematic diagram of the antipolar distortion. (f) Atomic displacement of the O_A in Ru(1) ion. All data are extracted from the previous neutron-scattering results [2,3].

To investigate the coupling between the phonon and the phase transition at T_{OO}, we perform DFT calculations. The phonon eigenmodes are calculated by the frozen phonon method. The eigenmode of the lowest A_g mode is shown in Figs. 4(a) and 4(b); we display only four neighboring RuO_6 octahedra, omitting the motions of Ca^{2+} because the cations with fully occupied electron shells hardly influence the optical responses. The A_g mode can be described by octahedral tilting associated with motions of both in-plane oxygen (O_P) and apical oxygen (O_A). The motion of O_P tilts along the a axis. However, we find that O_A vibrates along the $-x$ [$+y$] direction at the site of the Ru(1) [Ru(2)] ion. The diagonal motion of O_A in Ca_2RuO_4 is unusual, distinct from O_A motions in usual A_g phonon modes of a tilting character in

other layered compounds, which show rigid tilts of octahedral along the unit-cell axis [32,33].

We find that the O_A position of Ca_2RuO_4 qualitatively becomes different across T_{OO}. We closely examined the crystal structure associated with O_A. Figures 4(c) and 4(d) show simplified diagrams of the octahedral distortions, which are obtained from a close scrutiny of the previously reported neutron-scattering experiments at 295 and 180 K [2,3]. The octahedral rotations around the c axis are ignored in the diagrams for simplicity. The O_A positions at 295 K ($> T_{OO}$) represent usual octahedral tilting but with a discrepancy in tilting angles O_A and O_P. The O_A tilting angle (θ_A) is smaller than the O_P tilting angle (θ_P). As a result, when projected normally to the local O_P planes, O_A is shifted from the symmetric center positions in the $-a$ [$+a$] direction at the Ru(1) [Ru(2)] site, respectively, as shown in Fig. 4(c). However, the O_A positions at 180 K ($< T_{OO}$) are shifted along the diagonal directions along $-x$ [$+y$] in Ru(1) [Ru(2)] octahedral as depicted in Fig. 4(d). This contrasts clearly with the 295 K structure.

The discrepancy between the 180 and 295 K structures can be understood by an additional antipolar distortion of O_A toward the b axis, as shown in Fig. 4(e). The 180 K structure can be obtained if the antipolar distortion is added to the structure at 295 K. This results in site-dependent local anisotropy below T_{OO}. The neutron-scattering data available at four temperatures [2,3] indicate that the antipolar distortion develops around T_{OO} as shown in Fig. 4(f). The relative displacement of O_A at the Ru(1) [Ru(2)] site is almost pure Δx [Δy] at 180 K below T_{OO}, while the Δx and Δy components are comparable at 295 K above T_{OO}. Indeed, the tilting angle of O_A increases more steeply than O_P below 260 K (see Fig. 6 in Ref. [3]), which might be attributed due to the development of the antipolar distortion. We note that the O_A distortions from the symmetric position at 180 K are exactly parallel to the apical motions of the lowest A_g phonon mode. Therefore, it is natural that the phonon oscillations are sensitive to the temperature-dependent octahedral deformation. We suggest that the change of the position of the apical oxygen may result in a sign change in either of δQ or $(\partial R/\partial Q)$. Verifying the exact origin of the phase flip in Ca_2RuO_4 requires additional time-resolved measurement on the lattice structures, using x-ray pump-probe spectroscopy.

In summary, we investigate the coherent phonon oscillations in Ca_2RuO_4 that show a 180° phase variation across $T_{OO} = 260$ K. Careful inspection of the crystal structure provides evidence of structural evolution of octahedra with the development of antipolar distortion below T_{OO}. These observations put cornerstones to understand the mysterious 260 K transition in Ca_2RuO_4. Our results emphasize that phase-sensitive measurements of coherent oscillations offer a unique opportunity to investigate quantum phase transitions coupled to the lattice in complex materials.

This work was supported by the Institute for Basic Science (IBS) in Korea (IBS-R009-D1). K.W.K. was supported by the Basic Science Research Program through the National Research Foundation of Korea (NRF) funded by the Ministry of Science, ICT and Future Planning (NRF-2015R1A2A1A10056200 and 2017R1A4A1015564). J.K. and S.Y. were supported by NRF-2016R1D1A1B01009032. This work was supported by Japan Society for the Promotion of Science (JSPS) Grants-in-Aid for Scientific Research (KAKENHI) (No. JP15H05852, No. JP15K21717, and No. JP17H06136), JSPS Core-to-Core program. C.S. acknowledges support of the JSPS International Research Fellowship (No. JP17F17027).

[1] S. Nakatsuji, S. I. Ikeda, and Y. Maeno, J. Phys. Soc. Jpn. **66**, 1868 (1997).
[2] O. Friedt, M. Braden, G. André, P. Adelmann, S. Nakatsuji, and Y. Maeno, Phys. Rev. B **63**, 174432 (2001).
[3] M. Braden, G. Andre, S. Nakatsuji, and Y. Maeno, Phys. Rev. B **58**, 847 (1998).
[4] A. Jain, M. Krautloher, J. Porras, G. H. Ryu, D. P. Chen, D. L. Abernathy, J. T. Park, A. Ivanov, J. Chaloupka, G. Khaliullin, B. Keimer, and B. J. Kim, Nat. Phys. **13**, 633 (2017).
[5] T. Mizokawa, L. H. Tjeng, G. A. Sawatzky, G. Ghiringhelli, O. Tjernberg, N. B. Brookes, H. Fukazawa, S. Nakatsuji, and Y. Maeno, Phys. Rev. Lett. **87**, 077202 (2001).
[6] M.-C. Lee, C. H. Kim, I. Kwak, C. W. Seo, C. H. Sohn, F. Nakamura, C. Sow, Y. Maeno, E.-A. Kim, T. W. Noh, and K. W. Kim, arXiv:1712.03028.
[7] I. Zegkinoglou, J. Strempfer, C. S. Nelson, J. P. Hill, J. Chakhalian, C. Bernhard, J. C. Lang, G. Srajer, H. Fukazawa, S. Nakatsuji, Y. Maeno, and B. Keimer, Phys. Rev. Lett. **95**, 136401 (2005).
[8] D. G. Porter, V. Granata, F. Forte, S. Di Matteo, M. Cuoco, R. Fittipaldi, A. Vecchione, and A. Bombardi, Phys. Rev. B **98**, 125142 (2018).
[9] R. Huber, F. Tauser, A. Brodschelm, M. Bichler, G. Abstreiter, and A. Leitenstorfer, Nature (London) **414**, 286 (2001).
[10] S. D. Brorson, A. Kazeroonian, J. S. Moodera, D. W. Face, T. K. Cheng, E. P. Ippen, M. S. Dresselhaus, and G. Dresselhaus, Phys. Rev. Lett. **64**, 2172 (1990).
[11] R. Mankowsky, A. Subedi, M. Först, S. O. Mariager, M. Chollet, H. T. Lemke, J. S. Robinson, J. M. Glownia, M. P. Minitti, A. Frano, M. Fechner, N. A. Spaldin, T. Loew, B. Keimer, A. Georges, and A. Cavalleri, Nature (London) **516**, 71 (2014).
[12] C. Kübler, H. Ehrke, R. Huber, R. Lopez, A. Halabica, R. F. Haglund, and A. Leitenstorfer, Phys. Rev. Lett. **99**, 116401 (2007).
[13] K. W. Kim, A. Pashkin, H. Schäfer, M. Beyer, M. Porer, T. Wolf, C. Bernhard, J. Demsar, R. Huber, and A. Litenstorfer, Nat. Mater. **11**, 497 (2012).
[14] S. Gerber, K. W. Kim, Y. Zhang, D. Zhu, N. Plonka, M. Yi, G. L. Dakovski, D. Leuenberger, P. S. Kirchmann, R. G. Moore, M. Chollet, J. M. Glownia, Y. Feng, J.-S. Lee, A. Mehta, A. F. Kemper, T. Wolf, Y.-D. Chuang, Z. Hussain, C.-C. Kao, B. Moritz, Z.-X. Shen, T. P. Devereaux, and W.-S. Lee, Nat. Commun. **6**, 7377 (2015).
[15] F. Schmitt, P. S. Kirchmann, U. Bovensiepen, R. G. Moore, L. Rettig, M. Krenz, J.-H. Chu, N. Ru, L. Perfetti, D. H. Lu, M. Wolf, I. R. Fisher, and Z.-X. Shen, Science **321**, 1649 (2008).

[16] H. Schäfer, V. V. Kabanov, M. Beyer, K. Biljakovic, and J. Demsar, Phys. Rev. Lett. **105**, 066402 (2010).
[17] M. Först, C. Manzoni, S. Kaiser, Y. Tomioka, Y. Tokura, R. Merlin, and A. Cavalleri, Nat. Phys. **7**, 854 (2011).
[18] D. Polli, M. Rini, S. Wall, R. W. Schoenlein, Y. Tomioka, Y. Tokura, G. Cerullo, and A. Cavalleri, Nat. Mater. **6**, 643 (2007).
[19] L. Dhar, J. A. Rogers, and K. A. Nelson, Chem. Rev. **94**, 157 (1994).
[20] H. J. Zeiger, J. Vidal, T. K. Cheng, E. P. Ippen, G. Dresselhaus, and M. S. Dresselhaus, Phys. Rev. B **45**, 768 (1992).
[21] T. E. Stevens, J. Kuhl, and R. Merlin, Phys. Rev. B **65**, 144304 (2002).
[22] A. V. Kuznetsov and C. J. Stanton, Phys. Rev. Lett. **73**, 3243 (1994)
[23] S. Nakatsuji and Y. Maeno, J. Solid State Chem. **156**, 26 (2001).
[24] J. H. Jung, Z. Fang, J. P. He, Y. Kaneko, Y. Okimoto, and Y. Tokura, Phys. Rev. Lett. **91**, 056403 (2003).
[25] See Supplemental Material at http://link.aps.org/supplemental/10.1103/PhysRevB.98.161115 for additional experimental and theoretical details.
[26] G. Kresse and J. Hafner, Phys. Rev. B **47**, 558 (1993).
[27] G. Kresse and D. Joubert, Phys. Rev. B **59**, 1758 (1999).
[28] Z. Fang, N. Nagaosa, and K. Terakura, Phys. Rev. B **69**, 045116 (2004).
[29] E. Gorelov, M. Karolak, T. O. Wehling, F. Lechermann, A. I. Lichtenstein, and E. Pavarini, Phys. Rev. Lett. **104**, 226401 (2010).
[30] H. Rho, S. L. Cooper, S. Nakatsuji, H. Fukazawa, and Y. Maeno, Phys. Rev. B **71**, 245121 (2005).
[31] S.-M. Souliou, J. Chaloupka, G. Khaliullin, G. Ryu, A. Jain, B. J. Kim, M. Le Tacon, and B. Keimer, Phys. Rev. Lett. **119**, 067201 (2017).
[32] R. E. Cohen, W. E. Pickett, H. Krakauer, and L. L. Boyer, Physica B **150**, 61 (1988).
[33] C. H. Sohn, M.-C. Lee, H. J. Park, K. J. Noh, H. K. Yoo, S. J. Moon, K. W. Kim, T. F. Qi, G. Cao, D.-Y. Cho, and T. W. Noh, Phys. Rev. B **90**, 041105 (2014).